Proceedings of the 4th World Congress on Momentum, Heat and Mass Transfer (MHMT'19)
Rome, Italy – April, 2019
Paper No. ICMFHT 110
DOI: 10.11159/icmfht19.110

CFD–DEM Modelling Approach of Particle–Liquid Food Flows in a Bent Pipe

Mohd Tarmizan Ibrahim[1], Heiko Briesen[1], Petra Först[1], Jörg Zacharias[2]
[1]Chair of Process Systems Engineering
Technical University of Munich
Gregor-Mendel-Str. 4, Freising, Germany
mohd.tarmizan@tum.de; heiko.briesen@mytum.de; petra.foerst@tum.de
[2]Corporate Research and Development
Krones AG
Böhmewaldstrasse 5, 93073 Neutraubling, Germany
Joerg.Zacharias@krones.com

Abstract **-** The conveying process of a food solid-liquid system in a bent horizontal pipe was investigated using the multiphase Computational Fluid Dynamics-Discrete Element Method (CFD–DEM) approach. The simulations were performed with commercial software tools, namely ANSYS Fluent and EDEM. The shape of the food particles was modelled as a cubic with a multi-sphere model, and a drag equation particle was used to consider also the effect of non-spherical particles. The simulations were performed for 5 mm size peach particle with different suspension flow velocities (0.3 and 0.8 m/s) and particle mass concentrations (5%, 10%, and 30%). The comparison between experimental and simulated particle velocity profiles demonstrated that, despite some quantitative discrepancies, the CFD–DEM modelling yielded a good agreement with the experimental data and could capture the experimental trends. In addition, this simulation approach could provide valuable information about particle flow properties such as velocity and position, that are difficult to measure experimentally.

Keywords**:** CFD–DEM, Food particle, Cube, Particle velocity, Non-spherical.

1. Introduction

Coupled computational fluid dynamics–discrete element method (CFD–DEM) simulation has potentially a very wide range of application and has gained increasing importance in the study of particle–laden flows. The CFD-DEM approach described in literature [1] has been largely applied for analysing the behaviour of particles in fluid systems such as those for gas fluidisation with particles, pneumatic conveying, drying, granulation, coating, blending, segregation, agglomeration and particle dispersion in solid and fluid. In addition, some research institutes and industrial companies have integrated this model in the early stages of the research and product development, achieving a great reduction of the experimentation costs [1].

This concept follows an Eulerian–Lagrangian approach, in which the particles are described as discrete entities and the second law of Newton and Euler are solved to track each particle, whereas the fluid phase is assumed as a continuous phase and its flow is described by the volume–averaged Navier–Stokes equation. The forces acting on a particle are gravity, interparticle collision contact and fluid–particle interaction. The momentum exchange between particle and fluid facilitates the coupling.

Unlike the works on the pneumatic transport of particles in pipes, there are still only a few studies about the food particle–fluid flow conveying system in them. Furthermore, only a few researchers have considered non-spherical particles in gas-solid flows. The particle shape plays an important role in determining the particle–fluid interactions and, consequently, the bulk fluid flow. A comprehensive review of the CFD–DEM modelling of non-spherical particles in a two-phase flow has been conducted in [2].

In this study, we used CFD–DEM method to investigate the food particles behaviour in a fluid flowing from a tubular heat exchanger system in bent pipes. The aim of this work was to perform numerical simulations with this coupled method and quantify its prediction capability for non-spherical food particles flowing in a horizontal pipe with a U-bend. This simulation approach could provide valuable parameters about the flowing particles, such as velocity, path line and position,

that are difficult to measure in experimentally. The simulated velocity profiles were also compared with those obtained from experiments [3].

2. Numerical models

The CFD–DEM simulations, based on the Eulerian–Lagrangian framework, were carried out using the commercial software tools Ansys FLUENT 17.0 and EDEM 2017.1. In this coupled approach, the motion of discrete particles and the fluid flow inside the pipe are determined by respectively solving the second laws of motion of Newton and Euler as used in DEM and the Reynolds–averaged Navier–Stokes (RANS) equations. This method, which is mostly used for simulating particles in a fluid, is known as a non-resolved approach. In this method, the particle sizes are considered smaller than the fluid mesh, thus, these particles are not resolved in the CFD simulation. The following assumptions were made: isothermal system; incompressible fluid; constant particle and fluid properties; no chemical reactions and no particle breakage.

2.1. Fluid phase

The RANS equations were used to describe the motion of the incompressible fluid with particles, as follows [4]:

$$\frac{\partial}{\partial t}\left(\alpha_f \rho_f\right) + \nabla \cdot \left(\alpha_f \rho_f \vec{u}_f\right) = 0 \tag{1}$$

$$\frac{\partial}{\partial t}\left(\alpha_f \rho_f \vec{u}_f\right) + \nabla \cdot \left(\alpha_f \rho_f \vec{u}_f \vec{u}_f\right) = -\alpha_f \nabla p_f + \nabla \cdot \alpha_f \bar{\bar{\tau}}_f + \vec{f}_{int} + \alpha_f \rho_f \vec{g} \tag{2}$$

$$\vec{f}_{in} = \frac{\sum_{i=1}^{n} \vec{F}_{in,i}}{V_{mesh}} \tag{3}$$

where $\vec{u}_f$ is the fluid velocity, ρ_f is the fluid density, α_f is the volume fraction of the fluid in each cell, p is the pressure, $\bar{\bar{\tau}}_f$ is the fluid viscous stress tensor, $\vec{g}$ is the acceleration due to gravity, $\vec{f}_{int}$ is the volumetric fluid–particle interaction forces applied in each CFD cell (source term due to the momentum exchange rate), n is the number of particle in a computational cell, V_{mesh} is the computational cell volume and $\vec{F}_{in}$ is the fluid-particle interaction force, which includes drag force, lift force and other possible fluid-particle interaction forces.

2.2. Solid phase

The translational and rotational motions of the particles, as the solid phase, were described in EDEM as follows [1]:

$$m\frac{d\vec{u}_p}{dt} = m\vec{g} + \sum_{j=1}^{k} \vec{F}_{c,j} + \vec{F}_{in} \tag{4}$$

$$\bar{\bar{I}}\frac{d\vec{\omega}_p}{dt} = \sum_{j=1}^{k} \vec{T}_j \tag{5}$$

where $\vec{F}_{c,j}$ is the contact force acting between particles and particles and wall, $\vec{F}_{in}$ is the interaction force (as mentioned in the Section 2.1), $\vec{u}_p$ and $\vec{\omega}_p$ are the linear and angular particle velocities, respectively, m is the particle mass, k is the number of particles or wall in interaction with a particle, $\bar{\bar{I}}$ is the particle moment of inertia and $\vec{T}$ is the torque acting on a particle, which can be determined as follows [1]:

$$\vec{T} = \sum_{j=1}^{k} \vec{r}_{c,j}\, \vec{F}_{cp,j} \tag{6}$$

where $\vec{r}_c$ and $\vec{F}_{cp}$ denote the vector pointing from the centre of mass of a particle to the contact point and the contact force between particles, respectively. A detail explanation of the torque calculation of the non-spherical particles can be found in [1].

2.3. Drag model

The hydrodynamic drag force ($\vec{F}_D$) acting on the non-spherical particle was modelled using the Di Felice [5] drag model as follows:

$$\vec{F}_D = \frac{1}{2} C_D A \rho_f \left|\left(\vec{u}_f - \vec{u}_p\right)\right| \left(\vec{u}_f - \vec{u}_p\right) \left(\alpha_f{}^{-\xi}\right) \tag{7}$$

$$\xi = 3.7 - 0.65 exp\left(-\frac{\left(1.5 - log_{10} Re_p\right)^2}{2}\right) \tag{8}$$

where C_D is the drag coefficient, A is the particle cross-section area normal to the fluid flow and $\vec{u}_p$ is the particle velocity. To consider the effect of the surrounding particles, this formulation includes a voidage function $\left(\alpha_f{}^{-\xi}\right)$, which is usually a simple exponential function based on the fluid volume fraction. The drag coefficient (C_D) from Ganser [6] was used in the following equation, which is a function of the particle orientation and sphericity (ψ):

$$C_D = \frac{24}{Re_p K_1}\left[1 + 0.11\left(Re_p K_1 K_2\right)^{0.6567}\right] + \frac{0.4305}{1 + {3305}/{Re_p K_1 K_2}} \tag{9}$$

Re_p is the particle Reynold number calculated on the basis of the equal volume sphere diameter and K_1 and K_2 are the shape factors for the non-spherical particles and are determined as follows:

$$K_1 = \left[\left(d_n/3d_p\right) + (2/3)\psi^{-0.5}\right]^{-1} \tag{10}$$

$$K_2 = 10^{1.8148(-log\psi)^{0.5743}} \tag{11}$$

where d_n is the equal projected area diameter, which is equivalent to the diameter of a circle with the same projected area as that of the non-spherical particle.

3. Simulation setup

A straight pipe with a length of 12 m and a 0.3 m long U-bend, as schematised in Fig. 1, was three-dimensionally modelled using the ANSYS DesignModeler. The computational domain was discretized into hexahedral meshes in Ansys Meshing, producing with 20,764 mesh elements with 27,246 nodes. Monodisperse food particles were fed into the pipe with the same initial velocity of the incoming fluid stream. The DEM time step was 30% of the Rayleigh time, and the CFD time step was 100 times longer. The parameters used in these simulations are summarised in Table 1.

The cubic particles were approximated in EDEM using the multi-sphere approach, where the overlapping spherical particles were fixed in position relative to each other along the major axis of symmetry, as shown in Fig. 2. The particle mass centre and moment of inertia were calculated automatically in EDEM. The contact detection and calculation of force between

the multi-sphere particles were based on detection of contact between the spherical elements. A detail explanation of the force and momentum calculation of the multi-sphere approach can be found in [1].

The phase coupled SIMPLE scheme [4] was used for pressure–velocity coupling. The least squares cell–based gradient method and the QUICK scheme [4] were adopted for calculating the gradient and the momentum, respectively. The method has a first and second order of accuracy in time and space, respectively. The fluid was introduced uniformly upstream from the inlet as a velocity-inlet boundary condition, the outlet was specified as a pressure outlet and no-slip boundary conditions were applied to the pipe walls. The convergence criterion was that all the residual for each variable was controlled at least below 10^{-3}, as recommended in [4].

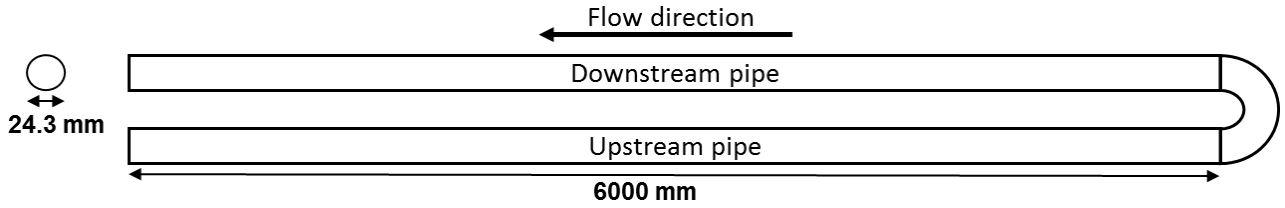

Fig. 1: Schematic diagram of the modelled pipe with the U-bend.

Table 1: Numerical parameters used for the simulations.

FLUENT	
Fluid type	Sugar solution
Fluid density (kg/m³)	1035
Fluid viscosity (Pa s)	0.00108
Viscous model	laminar
Inlet fluid velocity (m/s)	0.3 and 0.8
Time step (s)	1.0×10^{-3}
EDEM	
Initial particle velocity (m/s)	0.3 and 0.8
Poison's ratio	0.3
Particle-particle, particle-wall contact model	Hertz-Mindlin
Cubic particle side length (m)	0.005
Particle material	peach fruit
Particle density (kg/m³)	1035
Coefficient of restitution (particle-particle)	0.5
Coefficient of restitution (particle-wall)	0.5
Shear modulus (Pa)	1.0×10^{7}
Time step (s)	1.038×10^{-5}

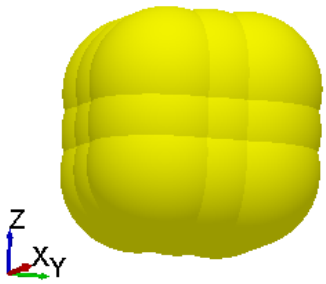

Fig. 2: Multi-sphere approach for modelling the cubic peach (particles as 27 spheres).

4. Results and discussion

In the previous electrical resistivity tomography (ERT) experiments [3], the particle velocity profile was measured at 20 points (on a symmetric line) of a pipe cross section after the bend. In the post–processing of EDEM simulation, the symmetric line (at the same position as in the experiments) was divided into 20 "grid bin" along the radial directions of the pipe, representing the sample points for the average particle velocity in the simulation. The velocity of a particle is determined as it passes through a particular grid bin, after the simulation time, an average velocity was computed for all particles that passed through the grid bins.

The experimental and simulated vertical profiles of the particle velocity along flow direction for an flow averaged velocity of 0.8 m/s are shown in Fig. 3., where the relative velocity is defined as the average particle velocity (v_p) divided by the average suspension flow velocity (w), and the relative position as the ratio of particle position from the pipe centre (r) to its inner diameter (D). In all cases, the model predicted particle velocities lower than the experimental values. However, a relatively flat average particle profile was obtained in the central parts of the pipe, which is a trend similar to that of the experimental results, but, the discrepancy between simulated and experimental profiles increased when getting closer to the pipe walls. A possible reason is that, the fluid mesh created for the CFD-DEM must be larger than the particle size, leading to a badly resolved fluid flow near the walls, and a consequent decrease of accuracy. The maximum deviations between simulations and experiments, at an average flow velocity of 0.8 m/s for particle mass concentrations of 5%, 10% and 30% were around 12%, 9% and 6%, respectively. Similar trends were also observed for an average flow velocity of 0.3 m/s, as shown in Fig. 4, with corresponding maximum discrepancies of about 10%, 9% and 7%. Overall, the simulation underestimated the particle velocity profiles. Nevertheless, the agreement can be considered reasonable considering the complexity of the two phases flow. One of the reasons for the discrepancy besides the comparable low mesh resolution could be the drag correlation model used: the Ganser [6] model was derived from a large number of experimental data about isometric particles and disc particles, which had a maximum mean relative error of 6.7%. Another reason could be the overestimation by 10% of the particle velocity profile by the ERT method from the particle tracking technique (high-speed camera), as investigated in [3].

Since the particle motion was described using Eulerian–Lagrangian approach, every particle attribute could be evaluated at a particular simulation time. We sampled the velocity and position of several particles at the upstream pipe end (before bend entrance) and at the downstream pipe beginning (after bend exit) from the simulation with the 0.3 m/s average flow velocity and the 10% particle concentration. The centrifugal force in the bend reduced the particle velocity magnitude from 5 to 13%, as shown in Fig. 5(a). Experimental work in [7] also showed that a maximum reduction between 8% and 15% of the particle velocity in the bend. The particle position illustrated in Fig. 5(b) looks altered because of the presence of a secondary fluid flow, for instance, particle 1 and 2 moved from the pipe centre towards the near pipe wall after travelling through the bend section, whereas, particle 4 moved inversely from the pipe wall towards the pipe centre after exiting the bend. Thus, changes in both velocity magnitude and position may affect the particle residence time in a pipe with a bend.

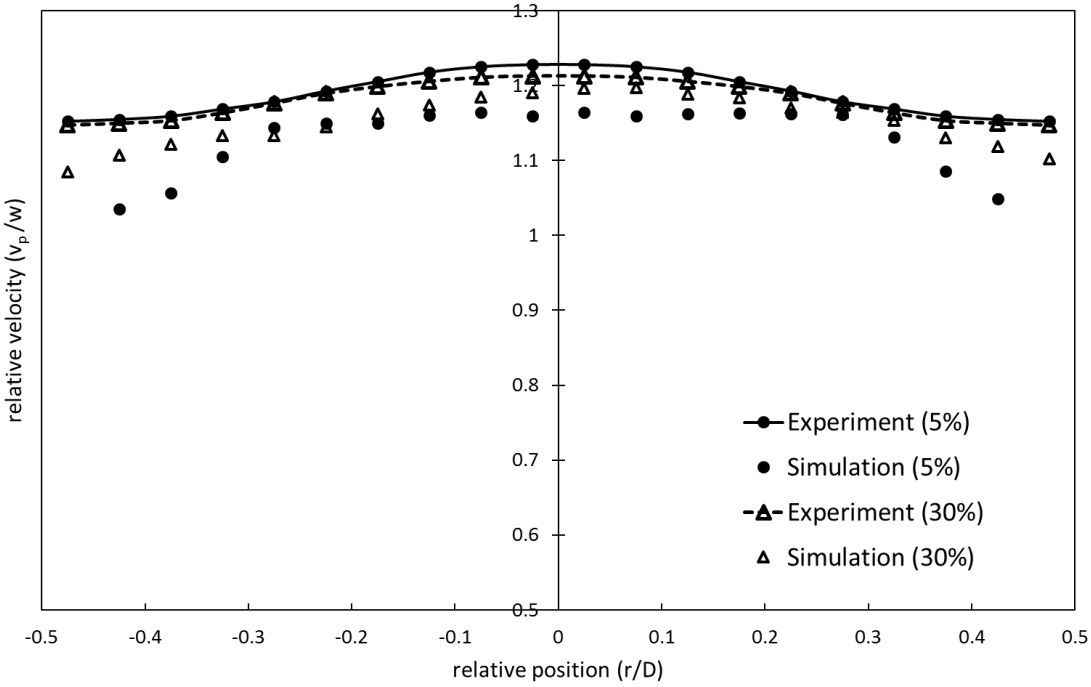

Fig. 3: Comparison between simulated and experimental particle velocity profiles for particle mass concentration of 5% and 30% and an average flow velocity of 0.8 m/s.

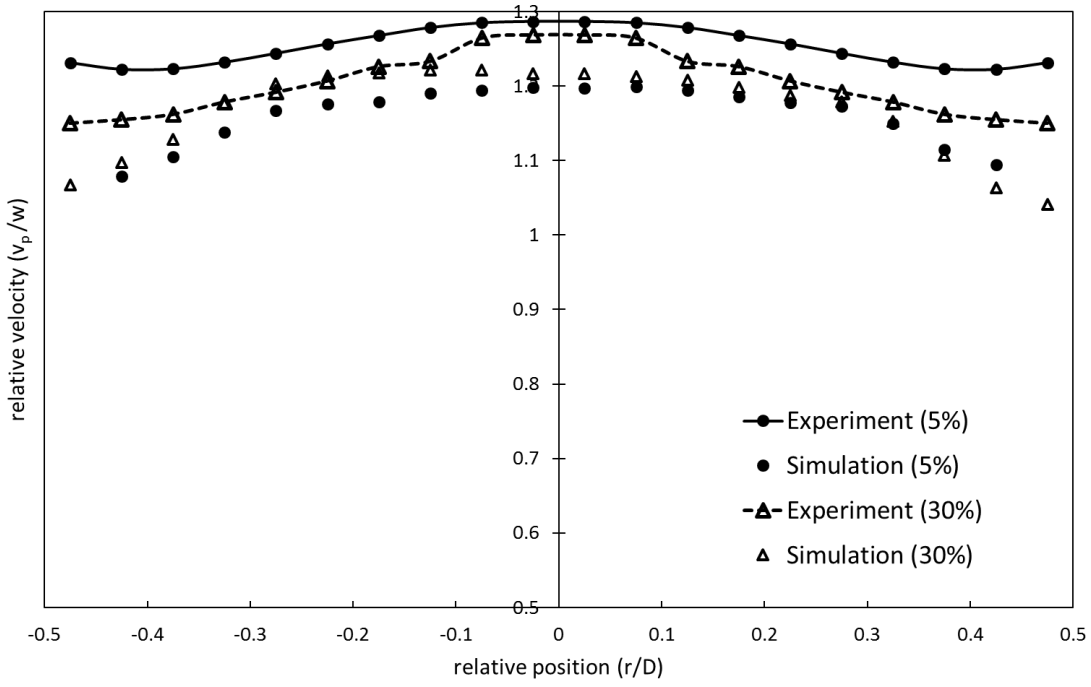

Fig. 4: Comparison between simulated and experimental particle velocity profiles for particle mass concentration of 5% and 30% and an average flow velocity of 0.3 m/s.

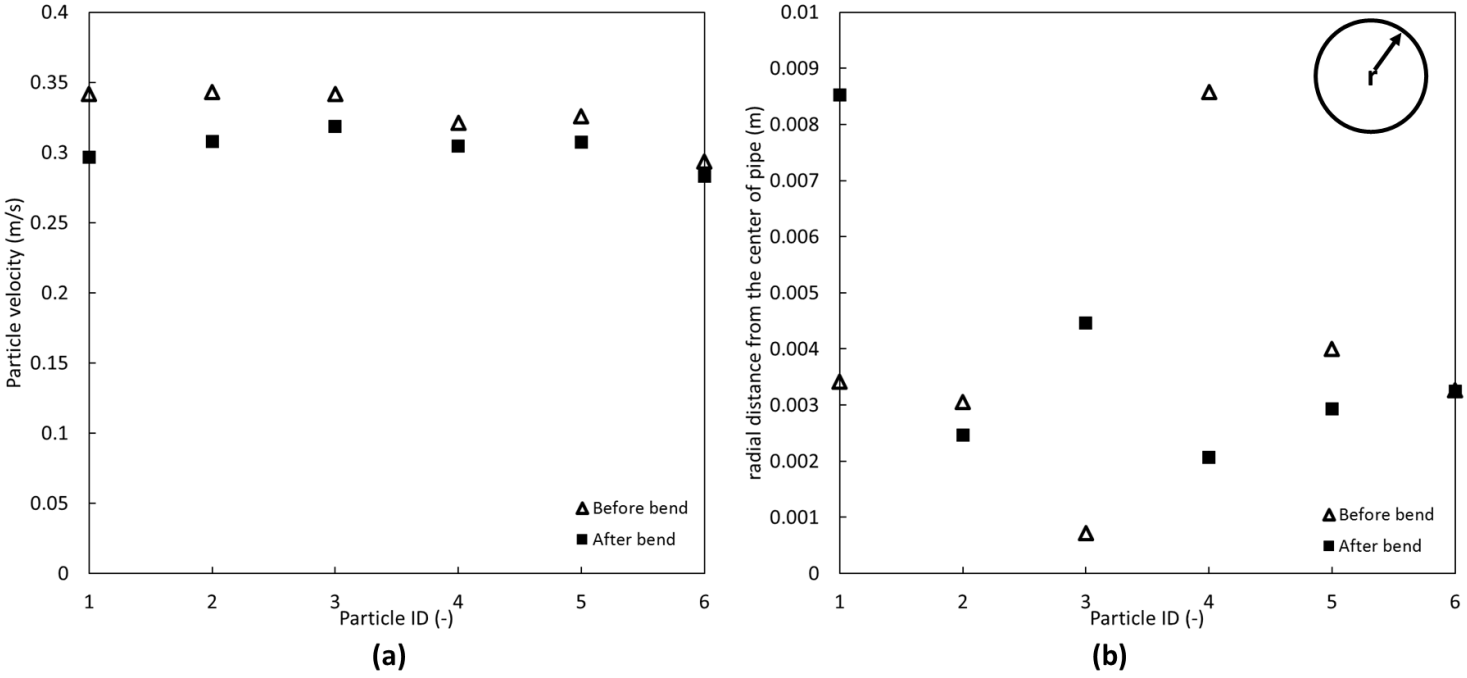

Fig. 5: Changes in the particle velocity (a) and radial position (b) before and after the bend; for an average flow velocity of 0.3 m/s and a particle mass concentration of 10%.

5. Conclusion

The flow of a solid-liquid dispersion in a straight pipe with a U-bend was investigated using the coupled CFD–DEM approach by means of the commercial software tools Ansys FLUENT and EDEM. The non-spherical food particles were modelled using a multi-sphere approach in EDEM. The CFD–DEM approach was able to qualitatively predict the particle flow profile in the pipe, as confirmed by experimental results. However, it consistently underestimated the particle velocity. The comparison between simulated and experimental results indicated the maximum discrepancies between 6% and 12%, which could be attributed to the errors reported in the chosen drag model or the errors from the ERT experiments. In the simulation, several particles were sampled to evaluate the effect of the bend on the particle velocity and motion.

CFD-DEM simulations can provide interesting information, especially on every particle, useful for the particulate liquid food process. Since several key particle parameters are obviously quite difficult to examine experimentally, this simulation tool could be very useful for determining and investigating the food particle path and residence time in a heat exchanger system. Further extensions of this model are currently being used to couple the flow simulation with energy equations for both phases.

References

[1] H. R. Norouzi, R. Zarghami, R. Sotudeh-Gharebagh, and N. Mostoufi, “CFD-DEM Applications to Multiphase Flow,” in *Coupled CFD-DEM Modeling*, Wiley-Blackwell, 2016, pp. 341–371.

[2] W. Zhong, A. Yu, X. Liu, Z. Tong, and H. Zhang, “DEM/CFD-DEM Modelling of Non-spherical Particulate Systems: Theoretical Developments and Applications,” *Powder Technol.*, vol. 302, pp. 108–152, 2016.

[3] T. Schweiger, “Untersuchung des Verweilzeitverhaltens und der Strömungsgeschwindigkeit grobdisperser Partikel in Röhrenwärmetauschern mittels ERT Tomographie,” Technische Universität München, Freising, DE, 2017.

[4] ANSYS Inc, “Fluent 17.0 user guide,” 2015.

[5] R. Di Felice, “The voidage function for fluid-particle interaction systems,” *Int. J. Multiph. Flow*, vol. 20, no. 1,

pp. 153–159, 1994.
[6] G. H. Ganser, “A rational approach to drag prediction of spherical and nonspherical particles,” *Powder Technol.*, vol. 77, no. 2, pp. 143–152, 1993.
[7] S. Grabowski and H. S. Ramaswamy, “Bend-effects on the residence time distribution of solid food particles in a holding tube,” *Can. Agric. Eng.*, no. 40, pp. 121–126, 1998.